VISUALIZATION STUDIES OF VISCOELASTIC FLOW IN A 4:1 SQUARE/SQUARE CONTRACTION

M. A. Alves
Departamento de Engenharia Química, CEFT, Faculdade de Engenharia da Universidade do Porto, Rua Dr. Roberto Frias s/n, 4200-465 Porto, Portugal
mmalves@fe.up.pt

D. Torres, M. P. Gonçalves
REQUIMTE/Departamento de Engenharia Química, Faculdade de Engenharia da Universidade do Porto, Rua Dr. Roberto Frias s/n, 4200-465 Porto, Portugal
pilarg@fe.up.pt

P. J. Oliveira
Departamento de Engenharia Electromecânica, Universidade da Beira Interior, 6201-001 Covilhã, Portugal
pjpo@ubi.pt

F. T. Pinho
Centro de Estudos de Fenómenos de Transporte, DEMEGI, Faculdade de Engenharia da Universidade do Porto, Rua Dr. Roberto Frias s/n, 4200-465 Porto, Portugal
fpinho@fe.up.pt

Abstract. Visualizations of the 3-D flow in a 4:1 sudden square-square contraction for a viscoelastic shear-thinning fluid under conditions of negligible inertia show provocative flow patterns. Whereas for a Newtonian fluid the vortex length remains unchanged, with the non-Newtonian fluid there is a dramatic increase in vortex length with fluid elasticity leading to unstable periodic flow at higher flow rates. In the steady flow regime the vortices are not closed and fluid particles enter the middle-plane vortex, rotate towards its eye, drift to the corner plane vortex, rotate to its periphery and exit to the downstream duct, a dynamic process that is opposite that found with Newtonian fluids. The periodic flow was characterised by a constant Strouhal number of 0.5.

Keywords: viscoelastic fluid, rheology, visualization, 3D 4:1 contraction flow

1. Introduction

Flow visualizations have always been important in fluid mechanics and it is one of the joys of the discipline, as illustrated in Van Dyke's (1982) classical work "An Album of Fluid Motion". They provide immediate understanding of many phenomena, enlightening elaborate mathematics. Non-Newtonian fluids are usually more viscous than common Newtonian fluids and their flows are frequently investigated by flow visualization since they are in the laminar regime. A similar compilation of non-Newtonian flow visualizations was written more recently by Boger and Walters (1993), which is a representative sample of the works published in this important subject of fluid mechanics.

Sudden contraction flows are classical benchmark problems used in computational rheology (Hassager, 1988), and a large number of visualization studies in planar and axisymmetric contractions are reported in the literature. The flow behaviour of non-Newtonian fluids in this simple configuration can be very surprising, and different flow patterns are observed even for fluids with similar rheological behaviour.

For viscoelastic fluids, the first visualizations were carried out by Cable and Boger (1978a, 1978b, 1979) and Nguyen and Boger (1979) who reported a dramatic growth of the salient corner vortex for shear rates above the critical value above which the normal stress grew quadratically. These experiments were performed for contraction ratios in the range 7.67:1 to 14.83:1. At much higher Weissenberg numbers, the ratio of fluid to flow characteristic times and thus a measure of flow elasticity, the flow became asymmetric and eventually time-dependent. In 1986 Boger et al investigated the behaviour of Boger fluids having similar steady and dynamic shear properties and yet found different vortex dynamics: they were thus forced to conclude that a different fluid property had to be taken into account. In his 1987 review paper, Boger suggested extensional viscosity as that property. For some fluids only a corner vortex exists which grows in size as elasticity increases. For other fluids the corner vortex extends to the reentrant corner and a lip vortex forms. As the elasticity increases the lip vortex grows at the expense of the corner vortex, while the length of the recirculation remains fairly constant. Eventually, the lip vortex occupies the whole region and a further increase in the Weissenberg number leads to an increase of the now concave shaped vortex. At higher Weissenberg numbers a small pulsating lip vortex appears and leads to unsteady behaviour.

In the mid 1980's and subsequently, the 4:1 contraction became the focus of a variety of experimental and numerical works aimed at various objectives. The experimental work concentrated on the investigation of the various flow transitions and instabilities and used several experimental techniques. The numerical work was unable to predict correctly the sub-critical steady flows and thus concentrated on improving the numerical techniques.

Soon after the beginning of the experimental investigations on axisymmetric contraction flows, the effect of different boundary conditions was also assessed. Flow in planar contractions were studied as early as 1982 by Walters and Webster who found no significant vortex activity in the 4:1 case with Boger fluids, in marked contrast to observations in 4.4:1 circular contractions. To help clarify these differences, Evans and Walters (1986) forced shear-thinning elastic fluids through various planar contractions (contraction ratios of 4:1, 16:1 and 80:1) to find vortex enhancement even in the smaller contraction and its intensification with both contraction ratio and fluid elasticity. For the larger contraction, however, a lip vortex was seen and a growth mechanism similar to that found for circular dies was seen, whereas in the 4:1 contraction only the corner vortex was observed. In 1988 Evans and Walters looked at the behaviour of Boger fluids in the 4:1 contraction to find a small lip vortex but without a connected corner vortex. Both the corner and lip vortices were reduced and here fluid inertia played a critical role. This independence of lip and corner vortices has also been found numerically as shown by Alves et al (2003) for Boger fluids represented by the Oldroyd-B model.

The surprising different behaviour of Boger fluids in circular and planar contractions has been recently confirmed by the careful experiments of Nigen and Walters (2002): experiments were conducted with both Newtonian and Boger fluids having identical shear viscosities and it is quite clearly demonstrated that, although higher extensional strain rates were found in the planar geometry than in the circular die, virtually no vortex enhancement was found in the former geometry whereas dramatic vortex enhancement for the Boger fluids was found in the latter.

Flow in square-square contractions has captured less attention but by no means it is unknown: Walters and Webster (1982) basically found similarities between the flows through circular and square-square contractions and the differences between the flows in planar and circular contractions were also confirmed by Walters and Rawlinson (1982) to occur also between planar and square-square 13.3:1 contractions. The experiments and numerical calculations of Purnode and Crochet (1996) also confirmed the similarities between the main flow features in 2-D and 3-D flows, and they concluded that lip vortices should not be associated with inertia effects. However, they also found that full capture of three-dimensional effects requires 3-D computations and especially an accurate representation of fluid rheology.

Nevertheless, it is clear that much less is known for the square-square contraction. The increase in computational power over the last few years has now made possible reasonably accurate numerical simulations of true 3D flows, for which there is a lack of experimental data for validation and this flow is an excellent candidate for such studies. This is the motivation for the present experimental work where visualizations of the flow patterns of a viscoelastic fluid in a 4:1 square/square contraction were carried out.

In the next Section the experimental apparatus is described, the rheology of the fluids is discussed and finally the flow visualizations are presented in Section 3 before the closure of the paper.

2. Experimental conditions

2.1. Experimental rig

The experimental apparatus is schematically depicted in Fig. (1). It consisted of two square ducts of length 1000 mm and 300 mm having sides of 24 mm and 6 mm, thus defining the 4:1 contraction ratio. Control of the flow was ensured by an adequate control of applied pressure on the upstream side of the rig and frictional losses in the long coiled pipe located at the bottom of the rig. To achieve low flow rates this coiled 8 m long pipe had a diameter of 4 mm, whereas for larger flow rates a larger 6 mm diameter pipe was used. Applied pressure was kept between 0.5 and 4 bar and the dashed lines represent pressurised air lines. The flow rate was measured by a stop-watch and the passage of the liquid free-surface at two marks in the upper duct.

The rig allows measurements in both the sudden contraction (valves V3 and V6 closed) and sudden expansion configurations (valves V4 and V5 closed), but here only the sudden contraction flow visualizations are reported. In all tests the fluid temperature was measured and the fluid properties were taken from the rheometric master curves shown in the next section.

To visualize the flow a 10 mW He-Ne laser light source was employed: the beam passed through a cylindrical lens to generate a sheet of light illuminating highly reflective tracer particles suspended in the fluid. Their trajectories were recorded using long time exposure photography with a conventional camera (CANON EOS 300 with a macro EF100mm lens).

The rheological properties of the viscoelastic fluid were measured by an AR2000 rheometer from TA Instruments with a cone-plate geometry, which could measure the shear viscosity (η) and the first normal stress difference coefficient (Ψ_1) in steady shear flow, and the rigidity and loss moduli (G', G'') in dynamic shear flow.

2.2. Rheological characterisation of the fluids

Two fluids were investigated in this study: a viscous Newtonian fluid (91% glycerine + 7.5% water + 1.5% NaCl and 25 ppm of biocide, all by weight concentrations) and a shear-thinning viscoelastic fluid (500 ppm of PAA in 85% glycerin and 15% water) in order to illustrate how a combination of shear-thinning and elasticity can result in dramatic differences of flow pattern. This viscoelastic shear-thinning fluid is henceforth referred to as ST1 fluid. From measurements of the shear viscosity (η) and first normal stress difference coefficient (Ψ_1) at various temperatures it

was possible to build master curves using the time-temperature superposition principle. The master-curves are represented in Figs. (2) and (3), respectively. The reduced rheometric data are defined as $\eta_r = \eta T_0 / a_T T$, $\Psi_{1,r} = \Psi_1 T_0 / a_T^2 T$ and $\dot{\gamma}_r = \dot{\gamma}\, a_T$, using a shift factor a_T as defined in Bird et al (1987)

$$a_T = \frac{\eta_0(T)\, T_0}{\eta_0(T_0)\, T} \tag{1}$$

It was found that an Arrhenius equation was able to correlate the temperature dependence of a_T with good accuracy:

$$\ln a_T = 6130\left(\frac{1}{T} - \frac{1}{T_0}\right) \tag{2}$$

where T_0 is the reference absolute temperature ($T_0 = 288.15\,\text{K}$).
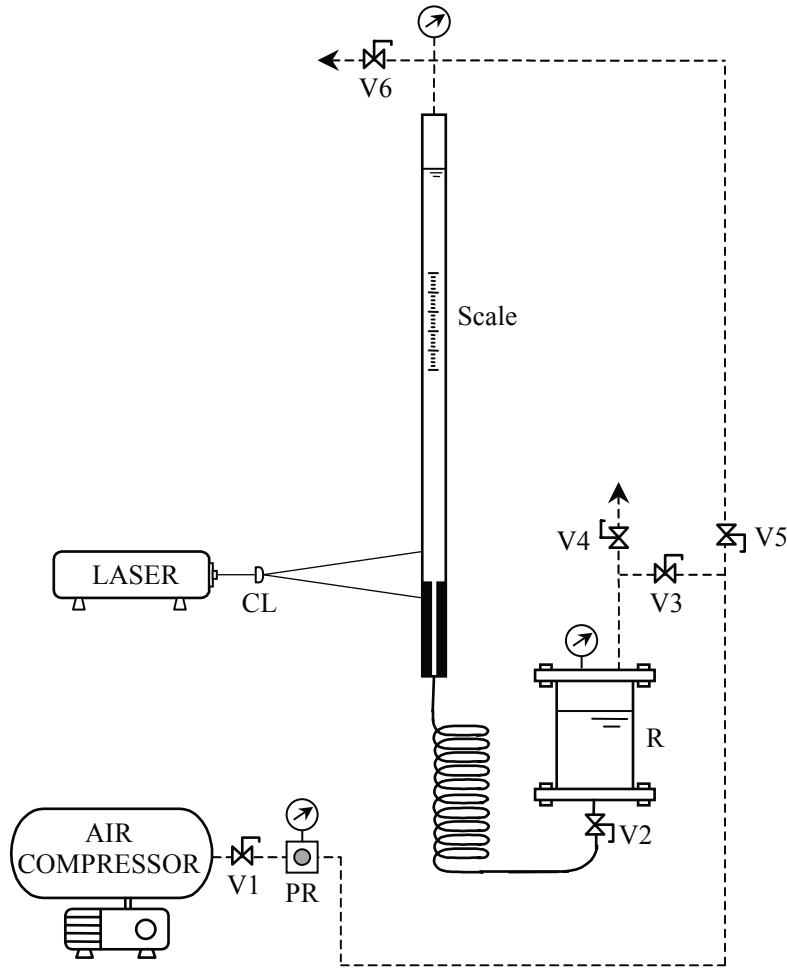
Figure 1. Schematic representation of the flow rig (PR- pressure regulator; V1 to V6- ball valves; R- reservoir; CL-cylindrical lens)

The ST1 fluid is shear-thinning with its viscosity showing the first Newtonian plateau at low shear rates, an asymptotic variation towards the second Newtonian plateau at high shear rates and an intermediate power law region with a power index of around 0.46. In the measured range the first normal stress difference coefficient is also shear-thinning, varying inversely with the shear rate and a comparison between Figs (2) and (3) shows the fluid to be highly elastic with N_1/τ_{xy} increasing from around 7 at $\dot{\gamma} = 10\ \text{s}^{-1}$ to around 12 at $\dot{\gamma} = 100\ \text{s}^{-1}$.
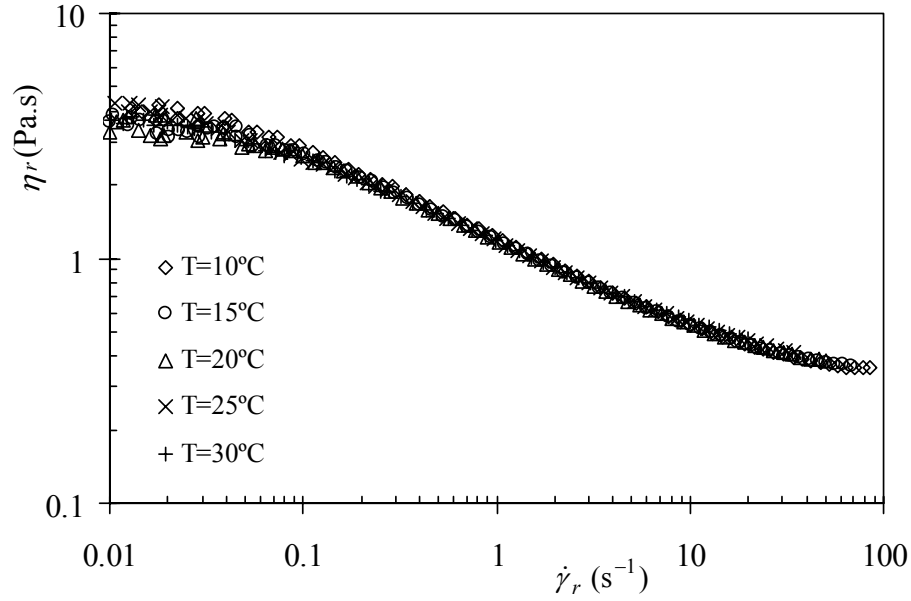
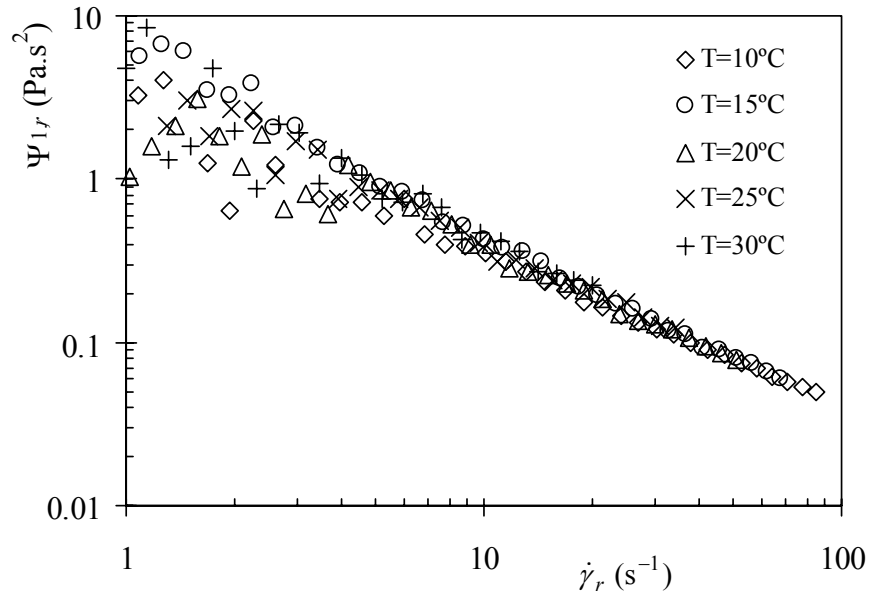Figure 2. Shear viscosity versus shear rate master curve for fluid ST1.

Figure 3. First normal stress coefficient versus shear rate master curve for fluid ST1.

3. Flow visualization results

3.1. Newtonian fluid

Flow visualizations were carried out first with Newtonian fluids for which there is a reasonable amount of knowledge (Boger, 1987) and here comparisons were also carried out with results of numerical simulations as is shown in Fig (4). The numerical results, not to be detailed here, were obtained with a finite-volume code developed by the authors (Alves et al, 2003). Figure (4), and all flow visualization figures henceforth represent stream-traces in the middle plane of the geometry. Even though the flow inside the vortex looks 2-D in reality it is 3-D and in contrast with real 2-D flows none of the vortices are ever closed.

In order to understand the descriptions of the Newtonian and non-Newtonian 3-D vortex flows let us consider two different vertical planes: the middle plane perpendicular to the wall (passing through points A-B, see Fig. (5)), which is always represented in the photos, and the second plane at 45° to the wall and passing through opposite corners of the

square cross-section (e.g. points C-D in Fig. (5)). In this second plane, henceforth referred as corner plane, no pictures could be taken.

When the fluid is Newtonian the fluid particles enter the vortex at the corner plane, they rotate towards the centre of the corner-plane vortex and then drift towards the eye of the middle-plane vortex. Once the particles are in the middle-plane vortex they rotate towards its periphery and exit the vortex at the reentrant corner going into the downstream duct, thus giving the impression that in this plane this vortex is closed. The sketch of Fig. (5) helps to understand this description.

The streamlines in the middle-plane vortex, obtained numerically, are also shown on the right-half of Fig. (4) and help to understand the dynamics inside this vortex; in the corner-plane vortex the opposite is happening. At low flow rates/Reynolds numbers inertial forces are negligible and the length of the vortex (x_R) is $x_R/H_1 = 0.33$, where H_1 represents the upstream duct half-width. As inertia becomes non-negligible the size of the vortices decrease with Reynolds number and eventually it almost vanishes at large flow rates.
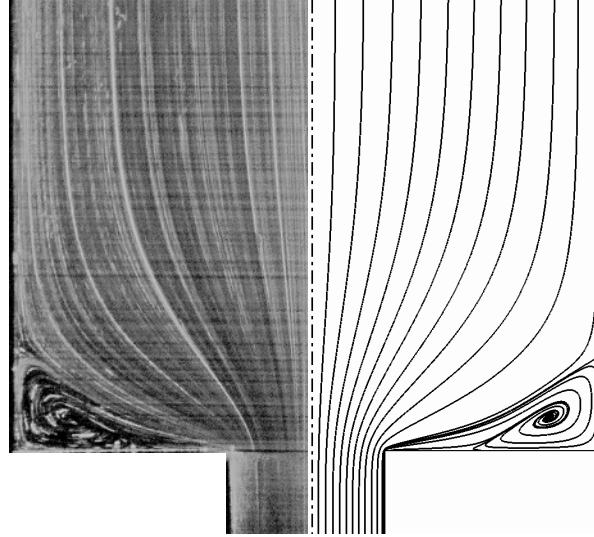

Figure 4. Newtonian contraction flow in the middle plane under conditions of negligible inertia ($Re= \rho U_1 H_1 / \eta = 0.0085$) and comparison with numerical results.
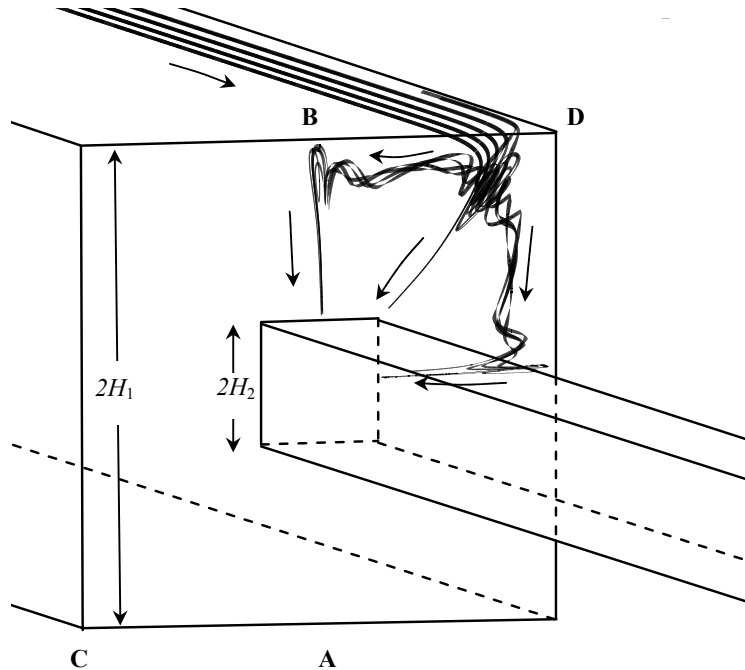

Figure 5. Sketch of particle trajectories in the vortices for a Newtonian fluid under negligible inertia.

3.2. Viscoelastic fluid

For the ST1 fluid the flow patterns are substantially different and depend on fluid elasticity as can be inferred in the various plots in Fig. (6). The strength of elasticity is quantified by the Weissenberg number $We = \lambda U / H$, where λ is the relaxation time of the fluid. Here, the Weissenberg number is not quantified because the flow characteristic shear rates fell outside the range of measured rheological data, but the implications of U on We are clear from the definition. Further rheological characterization of the fluid is required in order to determine the Weissenberg number but this is beyond the scope of this work.

In contrast to the Newtonian flow, the behaviour of ST1 is quite different and two flow regimes are identified, both under conditions of negligible inertia: at low flow rates (Weissenberg numbers) the flow is steady while at high flow rates it becomes unsteady but periodic. In all cases the flow is three-dimensional.

In the steady flow regime, represented in Fig. (6), we find the usual elastic vortex growth that is also present in plane and circular sudden contractions of shear-thinning fluids: as the flow rate increases from Fig. (6-a) to Fig. (6-e) the length of the vortex in the middle plane increases dramatically. At low flow rates (Fig. 6-a) the 3-D flow pattern has some similarities to that for the Newtonian fluid, although the vortex has already a slightly different shape: it is neither convex nor concave, whereas for the Newtonian fluid in Fig. (4) the eddy has a clear concave shape. We can also see that the middle plane vortex appears to be closed. However, at higher flow rates (Figs. 6-(b) to 6-(e)), when the flow is dominated by fluid elasticity and the vortex is longer, the pictures suggest a second dramatic change in flow pattern. We can not be fully conclusive on this issue, because the flow velocities were very low and it was not easy to follow visually a fluid particle to prove what we are about to describe. Hence the following arguments are partially speculative.

At higher flow rates the direction of motion of fluid particles inside the vortices is opposite to that found at lower flow rates and with Newtonian fluids. This is more clearly suggested in Figs. (6-c) and (6-d): the fluid coming from the upstream duct enters the middle-plane vortex (see some of the white streaks), rotates towards its eye and then moves towards the eye of the corner-plane vortex where it rotates from the eye towards its periphery and exits the corner-plane vortex to the downstream duct. This dramatic change remains a challenge for 3-D numerical simulations with viscoelastic models which can also help in understanding the true flow features but the use of symmetry planes is still possible to reduce computational effort.
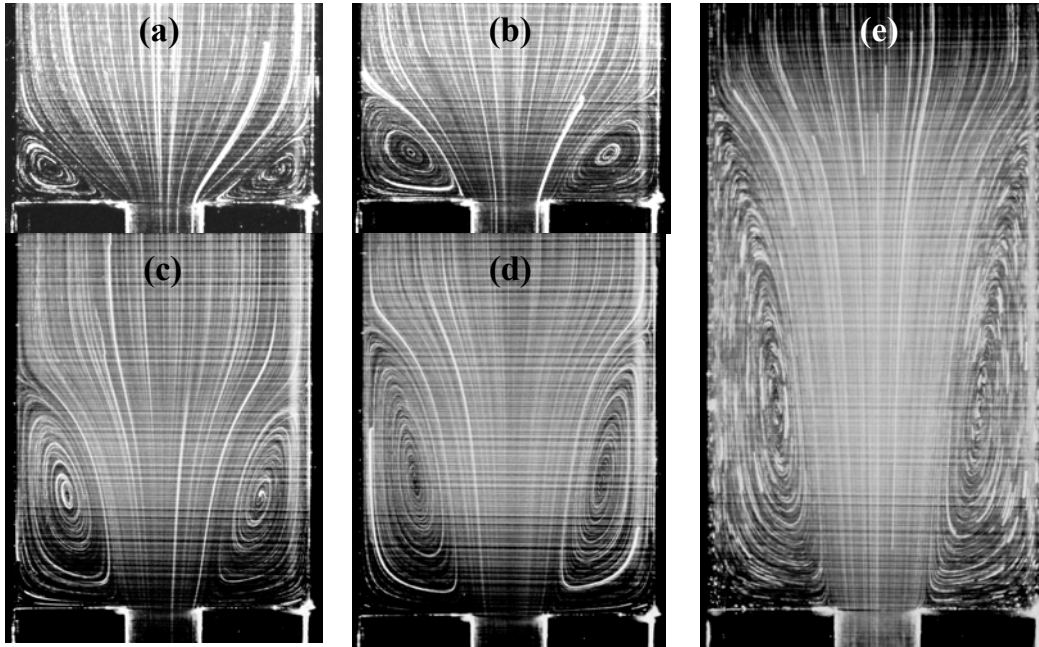

Figure 6. Corner vortex enhancement for fluid ST1 in a 4:1 square/square contraction: (a) U_1=0.00141cm/s; (b) U_1=0.00533 cm/s; (c) U_1=0.0208 cm/s; (d) U_1=0.0382 cm/s; (e) U_1=0.0783 cm/s.

The dramatic vortex growth is also seen in the plot of Fig. (7) representing the variation of the normalised vortex length (of the middle plane vortex) with the inlet bulk velocity. For velocities below 0.001 cm/s the size barely changes, but then its rate of change increases with flow elasticity and at about 0.1 cm/s the flow becomes periodic.

The sequence of pictures in Fig. (8) represents three different moments within a cycle of flow periodicity. Obviously, the periodicity is happening in both transverse directions. From films taken with a movie camera at a known frame rate it was possible to measure the frequency (f) of oscillation for different flow rates within the periodic regime and it was found that it varied linearly defining a constant Strouhal number $St = 2H_1 f / U_1 = 0.5$.

We speculate that at higher flow rates, not attained in these experiments, further elastic instabilities will grow and turn the flow chaotic. Predictions of the observed flow features will require a full 3-D, time-dependent simulation of the whole geometry with an adequate constitutive model, a challenge to be undertaken soon.
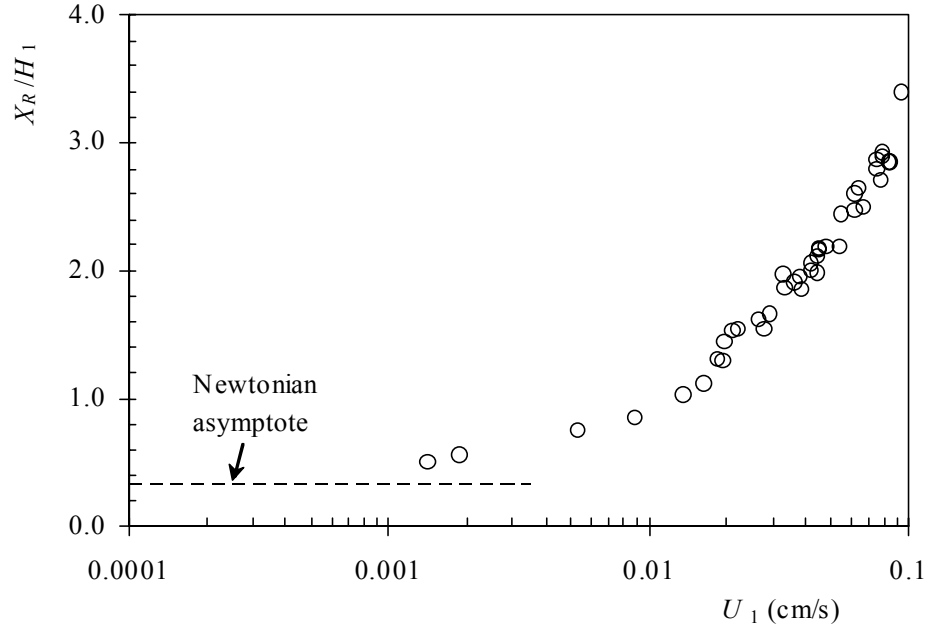

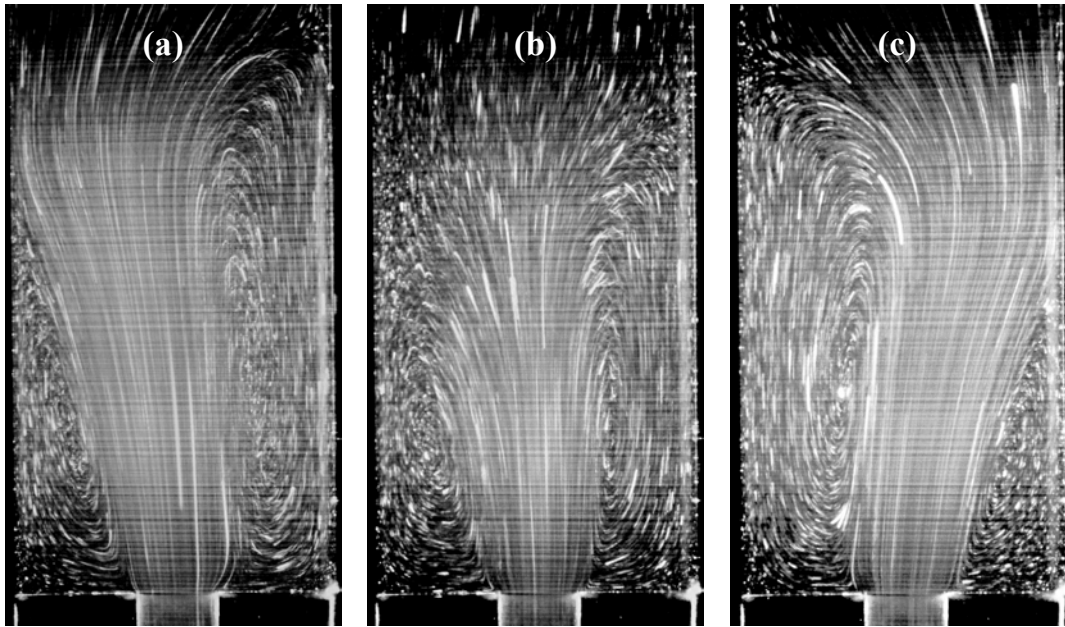Figure 7. Variation of normalised vortex length in the middle plane with the upstream bulk velocity.

Figure 8. Flow patterns for a super-critical shear rate for fluid ST1 (U_1=0.114 cm/s).

4. Conclusions

Flow visualizations were carried out in a 4:1 sudden square-square contraction for Newtonian and a viscoelastic shear-thinning fluid under conditions of negligible inertia. For the Newtonian fluid the flow pattern in the middle plane is in good agreement with numerical results. The flowfield is clearly three-dimensional with fluid particles moving from the upstream duct into the corner plane vortex, rotating towards the center and drifting to the middle plane vortex where they now rotate to the outside of the vortex and exit at the reentrant corner into the downstream duct. For the non-Newtonian fluid the visualizations suggest that provocative changes in fluid dynamics are taking place: the vortices

grew dramatically in size due to fluid elasticity and the dynamics inside the vortices have probably reversed with fluid particles entering the middle-plane vortex and exiting at the corner-plane vortex. At even higher flow rates the long vortices became unstable and a periodic flow was established.

5. Acknowledgements

6. References

Alves, M.A., Oliveira, P. J. and Pinho, F. T., 2003, "Benchmark solutions for the flow of Oldroyd-B and PTT fluids in planar contractions" J. Non-Newt. Fluid Mech., vol. 110, pp. 45-75.

Bird, R.B., Armstrong, R.C. and Hassager, O., 1987, "Dynamics of polymeric liquids. Volume 1: Fluid Dynamics", John Wiley & Sons, New York.

Boger, D.V., 1987, "Viscoelastic flows through contractions", Annual Rev. Fluid Mech., vol. 19, pp. 157-182.

Boger, D.V., and Walters, K., 1993, "Rheological Phenomena in Focus", Elsevier, Amsterdam.

Boger, D.V., Hur, D.U. and Binnington, R.J., 1986, "Further observations of elastic effects in tubular entry flows", J. Non-Newt. Fluid Mech., vol. 20, pp. 31-49.

Cable, P.J. and Boger, D.V., 1978a, "A compreensive experimental investigation of tubular entry flow of viscoelastic fluids: Part I. Vortex characteristics in stable flow. AIChEJ, vol. 24, pp. 868-879.

Cable, P.J. and Boger, D.V., 1978b, "A compreensive experimental investigation of tubular entry flow of viscoelastic fluids: Part II. The velocity fields in stable flow. AIChEJ, vol. 24, pp. 992-999.

Cable, P.J. and Boger, D.V., 1979, "A compreensive experimental investigation of tubular entry flow of viscoelastic fluids: Part III. Unstable flow. AIChEJ, vol. 25, pp. 152-159.

Evans, R.E. and Walters, K., 1986, "Flow characteristics associated with abrupt changes in geometry in the case of highly elastic liquids" J. Non-Newt. Fluid Mech., vol. 20, pp 11-29.

Evans, R.E. and Walters, K., 1988, "Further remarks on the lip-vortex mechanism of vortex enhancement in planar contraction flows" J. Non-Newt. Fluid Mech., vol. 32, pp. 95-105.

Hassager, O., 1988, "Working group on numerical techniques. Fifth International Workshop on Numerical Methods in Non-Newtonian Flows, Lake Arrowhead, USA" J. Non-Newt. Fluid Mechanics, vol. 29, pp. 2-5.

Nguyen, H. and Boger, D.V., 1979, "The kinematics and stability of die entry flows" J. Non-Newt. Fluid Mech., vol. 5, pp.353-368.

Nigen, S. and Walters, K., 2002, "Viscoelastic contraction flows: comparison of axisymmetric and planar configurations" J. Non-Newt. Fluid Mech., vol. 102, pp. 343-359.

Purnode, B. and Crochet, M. J. 1996, "Flows of polymer solutions through contractions. Part 1: flows of polyacrylamide solutions through planar contractions" J. Non-Newt. Fluid Mech., vol. 65, pp. 269-289.

Walters, K. and Rawlinson, D.M., 1982, "On some contraction flows for Boger fluids", Rheol. Acta, vol. 21, pp. 547-552.

Walters, K. and Webster, M.F., 1982, "On dominating elastico-viscous response in some complex flows", Phil. Trans. R. Soc. London A, vol. 308, pp. 199-218.

Van Dyke, M., 1982, "An Album of Fluid Motion", The Parabolic Press, Stanford, California.

7. Copyright Notice